



## Primary instabilities and bicriticality in fiber suspensions between rotating cylinders<sup>\*</sup>

WAN Zhan-hong<sup>†1</sup>, SUN Zhi-lin<sup>†‡1</sup>, YOU Zhen-jiang<sup>2</sup>

(<sup>1</sup>Department of Hydraulic and Ocean Engineering, Zhejiang University, Hangzhou 310028, China)

(<sup>2</sup>School of Informatics and Engineering, Flinders University of South Australia, Adelaide, SA 5001, Australia)

<sup>†</sup>E-mail: zhwansd@163.com; oceansun@zju.edu.cn

Received Feb. 21, 2007; revision accepted Apr. 25, 2007

**Abstract:** The linear stability of fiber suspensions between two concentric cylinders rotating independently is studied. The modified stability equation is obtained based on the fiber orientation model and Hinch-Leal closure approximation. The primary instabilities and bicritical curves have been calculated numerically. The critical Reynolds number, wavenumber and wave speeds of fiber suspensions as functions of the aspect ratio, volume concentration of the fibers and the gap width of cylinders are obtained.

**Key words:** Fiber suspensions, Primary instability, Non-axisymmetric disturbances

**doi:** 10.1631/jzus.2007.A1435

**Document code:** A

**CLC number:** TN929.5

### INTRODUCTION

The flow of fiber suspensions has been very popular in the industry as well as in theoretical research. Because the final product properties, such as mechanical, thermal and electrical performance, are highly sensitive to orientation distribution and spatial configuration of fibers, which are related to flow state in the industrial processing, some discussions on the issue of the instability occurring in fiber suspension flow between a pair of coaxial rotating cylinders have been made. The contribution of the added fibers to the bulk fluid can be macroscopically described by constitutive equations. So there are generally two main directions in the stability research aspect corresponding to constitutive models so far: (1) Transversely isotropic fluid (TIF) models. These models were variants of the continuum model originally derived by Ericksen (1960) and Hand (1962) and their micro-structure origins were recognized by Doi and Edwards (1978a; 1978b). Leslie (1964) explored

solution conditions under which there exist infinitesimal axially symmetric, stationary secondary flows and claimed that there is a range of conditions within which it is stable. Verma (1962) obtained an analytic solution of the Couette flow problem using Ericksen's constitutive equations. Ericksen (1966) considered stability with respect to arbitrary disturbances and resolved the discrepancy of conclusions drawn by Verma (1962) and Leslie (1964). Pilipenko *et al.* (1981) investigated the stability of small-gap Taylor-Couette flow using the model of an anisotropic Ericksen fluid, into which the values of the parameters entering are made specific in the case of weak Brownian motion. Nsom (1994) reported the results of the wide-gap Taylor-Couette configuration. The non-axisymmetric instability was studied by Wan *et al.* (2005) and the influences of the radii ratio of the inner and outer cylinders were further discussed. (2) Batchelor's model. The constitutive model of Ericksen or Hand is not a sufficiently general formation and only suited for some particular situations. Batchelor (1971), Hinch and Leal (1975; 1976), and Shaqfeh and Fredrickson (1990) developed a general constitutive equation for suspensions of fibers at ar-

<sup>‡</sup> Corresponding author

<sup>\*</sup> Project (Nos. 10632070 and 40231017) supported by the National Natural Science Foundation of China

bitrary concentrations. Based on this model, Gupta *et al.* (2002) carried out an instability analysis, with respect to axisymmetric disturbances, of semi-dilute non-Brownian suspension in conjunction with a quadratic and hybrid closure. We had known that, in a simple Taylor-Couette flow, the regions of crossover from Taylor vortices to spirals or between spirals of different azimuthal wavenumbers may exhibit more complex dynamics as a result of interaction of several modes of flow. In the present paper, we continue the previous work (Wan *et al.*, 2007) and give a comprehensive quantitative view of the possibilities for a wide range of cylinder radius ratios and for several azimuthal wavenumbers in fiber suspensions Taylor-Couette flow.

## THEORETICAL MODEL

Consider two infinitely long, concentric cylinders of radii  $R_1$  and  $R_2$  ( $0 < R_1 < R_2$ ), respectively. The flow occurred in the annulus between them. The cylindrical coordinate system  $(r, \theta, z)$ , with the  $z$  axis chosen as the common axis of the two cylinders, is used. The flow is driven by rotation of either one, or both, of the inner and outer cylinders, with the angular velocities  $\Omega_1$  and  $\Omega_2$ . The flow problem is characterized by three geometric, one kinetic and two flow dimensionless parameters: the ratio of the radii,  $\eta = R_1/R_2$ ; the dimensionless axial wavelength  $L = 2\pi/(kd)$  and the azimuthal wave angle  $\theta$ , where  $d = R_2 - R_1$  is the gap width, and  $k$  is the wavenumber corresponding to the assumed periodicity in the axial direction; the ratio of the angular velocities,  $\Omega = \Omega_2/\Omega_1$ ; the Reynolds numbers associated with the inner and outer cylinders are:

$$Re = R_1\Omega_1 d/v, Re_2 = R_2\Omega_2 d/v, \quad (1)$$

where  $v$  is the kinematic viscosity. The governing equations are brought into non-dimensional form by rescaling the lengths by the gap width  $d$ , the velocity  $\mathbf{u}$  by the inner cylinder velocity  $R_1\Omega_1$ , and time  $t$  by the momentum diffusion time  $\rho d^2/\mu$  across the gap and the pressure  $p$  by the quantity  $\rho R_1\Omega_1 v/d$ . The dimensionless equations are expressed as

$$\nabla \cdot \mathbf{u} = 0, \quad (2)$$

$$\frac{\partial \mathbf{u}}{\partial t} + Re(\mathbf{u} \cdot \nabla \mathbf{u}) = -\nabla p + \nabla \cdot \boldsymbol{\tau}, \quad (3)$$

$$Re^{-1} \frac{\partial \mathbf{a}_2}{\partial t} + \mathbf{u} \cdot \nabla \mathbf{a}_2 = -(\boldsymbol{\omega} \cdot \mathbf{a}_2 - \mathbf{a}_2 \cdot \boldsymbol{\omega})/2 + \chi(\dot{\boldsymbol{\gamma}} \cdot \mathbf{a}_2 + \mathbf{a}_2 \cdot \dot{\boldsymbol{\gamma}} - 2\mathbf{a}_4 : \dot{\boldsymbol{\gamma}})/2 + 2C_1 |\dot{\boldsymbol{\gamma}}| (\boldsymbol{\delta} - \alpha \mathbf{a}_2), \quad (4)$$

$$\mathbf{a}_4 = G(\mathbf{a}_2), \quad (5)$$

where  $\boldsymbol{\delta}$  is the unit tensor and  $\alpha$  is the dimension of space,  $C_1$  is the interaction coefficient, the tensor  $\boldsymbol{\tau}$  is the state of stress in the fluid,  $\mathbf{a}_2$ ,  $\mathbf{a}_4$  are the second- and fourth-order orientation tensors, respectively;  $G$  represents the closure approximation used to determine  $\mathbf{a}_4$ . So far, a number of closure models have been put forth to approximate the fourth-order tensor by a known second-order tensor. Popular closure approximations have been those of linear and quadratic type (Hand, 1962), the composite closure derived by Hinch and Leal (1975; 1976), hybrid closure (Advani and Tucker III, 1987), orthotropic approximation proposed by Cintra and Tucker (1995). Parsheh *et al.* (2006) studied the performance of different closure models in a planar contraction flow. Some models are particularly well suited to 2D flow situations. Since the Taylor-Couette instability leads to 3D secondary flow, in this study we still adopt the Hinch-Leal closure approximation similar to our previous paper (Wan *et al.*, 2007), with the relationship between the components of  $\mathbf{a}_4$  and those of  $\mathbf{a}_2$  being given by:

$$a_{ijkl} = [2(\delta_{ij} a_{kl} + a_{ij} \delta_{kl}) - a_{ij} a_{kl} + 3(a_{ik} a_{jl} + a_{il} a_{jk}) - 2(\delta_{ij} a_{km} a_{ml} + a_{im} a_{mj} \delta_{kl})]/5. \quad (6)$$

In Eq.(4),  $\dot{\boldsymbol{\gamma}}$ ,  $\boldsymbol{\omega}$  are the rate of strain tensor and the vorticity tensor respectively and are defined by

$$\dot{\boldsymbol{\gamma}} = \nabla \mathbf{u}^T + \nabla \mathbf{u}, \quad \boldsymbol{\omega} = \nabla \mathbf{u}^T - \nabla \mathbf{u}, \quad (7)$$

and  $\chi$  is related to the aspect ratio by the following expression:

$$\chi = (r_a^2 - 1)/(r_a^2 + 1), \quad (8)$$

in which  $r_a = L/d$  is the aspect ratio of the fiber. The stress of fiber suspensions in Eq.(3) consists of two parts: the contribution of the suspending fluid and that

of the fibers. Details are given by Azaiez (2000) and You *et al.*(2004).

Express the characteristic variables in the form of the fundamental profile plus a small disturbance:

$$\mathbf{u}(r, \theta, z, t)=[\mathbf{u}^*(r, \theta, z, t), V_0(r) + \mathbf{v}^*(r, \theta, z, t), \mathbf{w}^*(r, \theta, z, t)], \tag{9a}$$

$$\mathbf{p}(r, \theta, z, t)=\mathbf{p}_0(r)+\mathbf{p}^*(r, \theta, z, t), \tag{9b}$$

$$\mathbf{a}_2(r, \theta, z, t)=\mathbf{a}_{20}(r) + \mathbf{a}_2^*(r, \theta, z, t). \tag{9c}$$

The disturbance is expressed in the following normal mode form:

$$\mathbf{u}^*(r, \theta, z, t)=\mathbf{u}(r)\exp[\lambda t+i(m\theta+kz)], \tag{10}$$

where  $m$  is the wavenumber corresponding to the assumed periodicity in the azimuthal direction.

The temporal stability is discussed here, so the characteristic exponent  $\lambda(k, m)$  is in general complex and can be expressed as:

$$\lambda = \text{Re}\lambda + i\text{Im}\lambda = \sigma - i\omega, \tag{11}$$

where  $\sigma$  and  $\omega$  can be explained as the growth rate and the characteristic frequency of the disturbance with the physical interpretation of azimuthal wave speed in the  $k$ - $m$  plain, respectively. Other variables such as the pressure and orientation tensors can be expressed similarly. Substitution of these variables into Eqs.(2)~(4) and the linearization lead to a complex generalized eigenvalue problem of the type

$$\mathbf{U}\mathbf{X}=\lambda\mathbf{V}\mathbf{X}, \tag{12}$$

where the vector  $\mathbf{X}=(\mathbf{u}, \mathbf{p}, \mathbf{a}_2)$ . The zero-boundary conditions of the disturbances are applied at the cyl-

inder walls. The solution of Eq.(12) is obtained numerically using the Chebyshev spectral method (Orszag, 1971). The procedure includes two steps in general: first, the differential equation is replaced by a set of difference equations; second, the differentiation matrix operators proposed by Weideman and Reddy (2000) and Trefethen (2001) are applied to the differential equations. For every given value of fiber parameters and disturbance parameters, the complex eigenvalue  $\lambda$  is sought and the eigenvector  $\mathbf{X}$  may be obtained further, from which all the flow variables can be obtained.

### RESULTS AND DISCUSSION

The critical Reynolds number of the inner cylinder  $Re_c$  is defined as the smallest value of  $Re$  for which an unstable eigenmode exists. In the non-axisymmetric disturbances, the wavenumbers in the azimuthal direction of the critical disturbance are generally different. Among them, the disturbance wave with the smallest value of  $Re_c$  determines the instability of the flow. When the ratio of the angular velocity of the outer cylinder to that of the inner cylinder is non-negative ( $\Omega=\Omega_2/\Omega_1\geq 0$ ), the numerical results of fiber suspensions, analogous to the Newtonian flow, show that the most unstable mode always corresponds to an axisymmetric disturbance irrespective of the changes of the other parameters. However, this is not always correct for negative values of  $\Omega$ .

The comparisons between the Newtonian flow and fiber suspensions (aspect ratio  $r_a=10^2$ , volume fraction  $c=10^{-4}$ ) for different azimuthal wavenumber  $m$  with  $\eta=0.675$  are shown in Fig.1. The subscripts

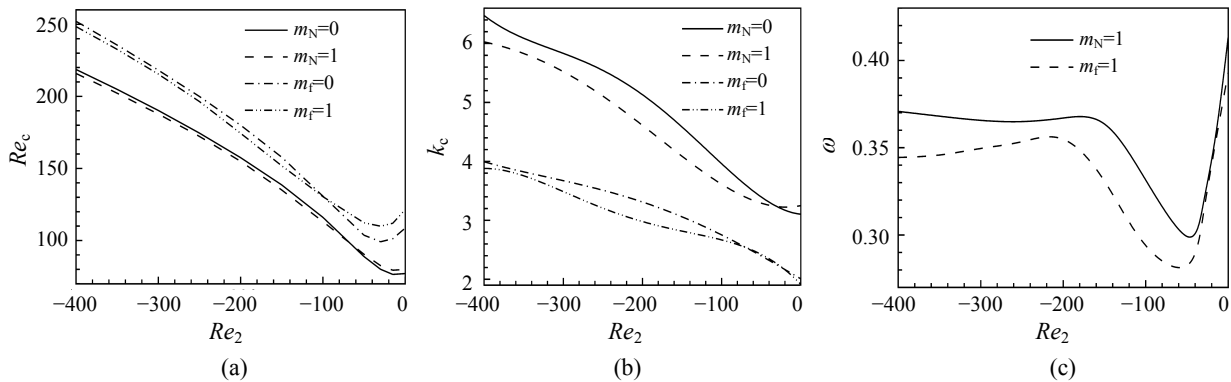


Fig.1 Comparisons between Newtonian flow and fiber suspensions. (a)  $Re_c \sim Re_2$ ; (b)  $k_c \sim Re_2$ ; (c)  $\omega \sim Re_2$

'N' and 'f' denote the Newtonian flow and fiber suspensions, respectively. The relationship between the critical inner Reynolds number  $Re_c$  and the outer Reynolds number  $Re_2$  is given in Fig.1a. It can be found that in both the Newtonian flow and fiber suspensions, two modes of different azimuthal wavenumbers become unstable simultaneously, given a large negative value of  $Re_2$ . Here, we refer to the crossing points as bicritical points. It is also obvious that the addition of fibers not only improves the value of  $Re_c$  signifying a stabilization effect for both axisymmetric and nonaxisymmetric disturbances, but also makes the bicritical points moving towards left. Fig.1b shows the critical axial wavenumber  $k_c$  as a function of  $Re_2$ . As known, the value of  $k_c$  increases with the absolute value of  $Re_2$  for different disturbance mode  $m$ . However, the critical axial wavenumber  $k_c$  of fiber suspensions is larger than that of the Newtonian flow for a fixed  $m$ . In Fig.1c we have the azimuthal wave speed  $\omega$  versus the outer Reynolds number  $Re_2$ . The wave speed  $\omega$  has been nondimensionized by  $m\Omega_1$  in order to examine the

extent to which the waves are dispersionless with respect to the azimuthal wavenumber. Thus, the wave speeds stay within a confined range. It comes out that the wave speed of the nonaxisymmetric disturbance modes in fiber suspensions has similar variant characteristics to that of the Newtonian flow. However, the wave speed of fiber suspensions is always smaller than that of the Newtonian flow. It implies that the resultant effect of fibers is to reduce the disturbances. When the absolute value of  $Re_2$  is relatively small, the wave speed changes significantly. Moreover, the influence of fibers on the wave speed is not evident. The larger absolute value of  $Re_2$  leads to the greater attenuation of the fibers on  $\omega$  and the smoother curve of the variation of the wave speed.

If we regard the Reynolds number of the inner cylinder  $Re$  as a continuous function of the outer Reynolds number  $Re_2$  and the axial wavenumber  $k$ , hence for a given  $Re_2$ , there exists an axial wavenumber  $k$ , where  $Re$  reaches its minimum. We refer to this axial wavenumber  $k$  as a critical axial wavenumber  $k_c$ . Figs.2~4 provide the critical inner

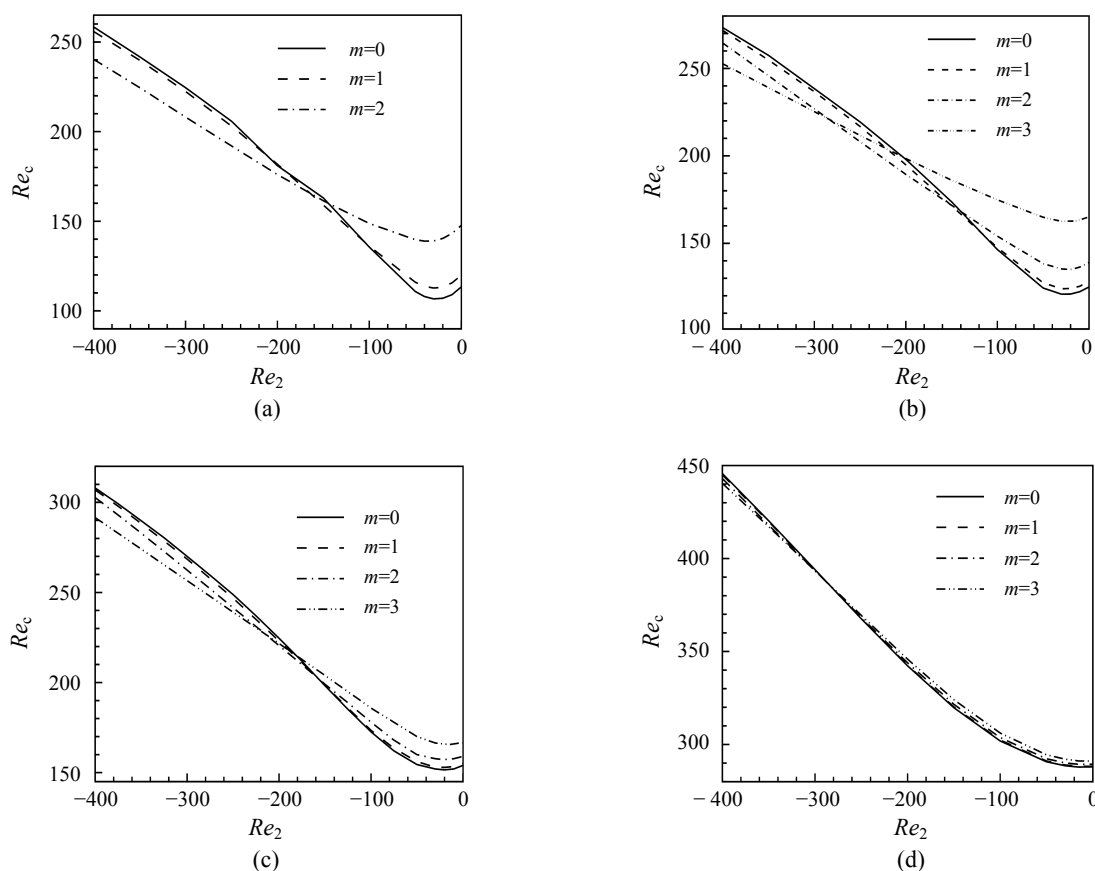


Fig.2 Relations between  $Re_c$  and  $Re_2$ . (a)  $\eta=0.750$ ; (b)  $\eta=0.825$ ; (c)  $\eta=0.900$ ; (d)  $\eta=0.975$

Reynolds number  $Re_c$ , the critical axial wavenumber  $k_c$  and the azimuthal disturbance wave speed  $\omega$  as functions of the outer cylinder  $Re_2$ , respectively. In each figure, the results of different radii ratio  $\eta$  and azimuthal wavenumber  $m$  are listed. The fiber parameters  $r_a=10^2$  and  $c=10^{-4}$  are fixed to obtain these results. As usual, the minimum of the critical Reynolds number of the inner cylinder  $Re_c$  determined the instability of the flow.

Fig.2 shows that, for a given outer Reynolds number  $Re_2$ , the difference of  $Re_c$  of the neighboring azimuthal disturbance modes becomes gradually smaller with the increase of the radii ratio  $\eta$ . It results in the curves overlapping each other and there are no evident cross points. Linking the lowest of the curves in each figure, we can obtain the predicted critical curve defined by the most unstable disturbance modes. For a given radii ratio, all the critical curves vary smoothly and there are no obvious jumps except that the slopes at the bicritical points have small differences.

From Fig.3 in conjunction with Fig.2, it can be seen that the critical axial wavenumber  $k_c$  changes discontinuously in the bicritical points where the azimuthal wavenumber  $m$  changes. Furthermore, the larger the azimuthal disturbance mode  $m$  is, the more pronounced the size of the discontinuity is. While the distance between two cylinders becomes very small, the critical axial wavenumber  $k_c$  corresponding to each azimuthal mode  $m$  monotonously increases with the rise of  $Re_2$ . The curves for each value of azimuthal wavenumber  $m$  get closer to one another and the jumps become unobvious.

The variations of the wave speed of the non-axisymmetric modes are shown in Fig.4. When the Reynolds number of the outer cylinder  $Re_2$  is relatively small, the wave speed of  $m$  mode is always smaller than that of  $m+1$  mode. Furthermore, the differences of the wave speeds among different non-axisymmetric modes are relatively small. But these differences gradually increase as  $Re_2$  becomes more negative and the wave speed of  $m$  mode gets

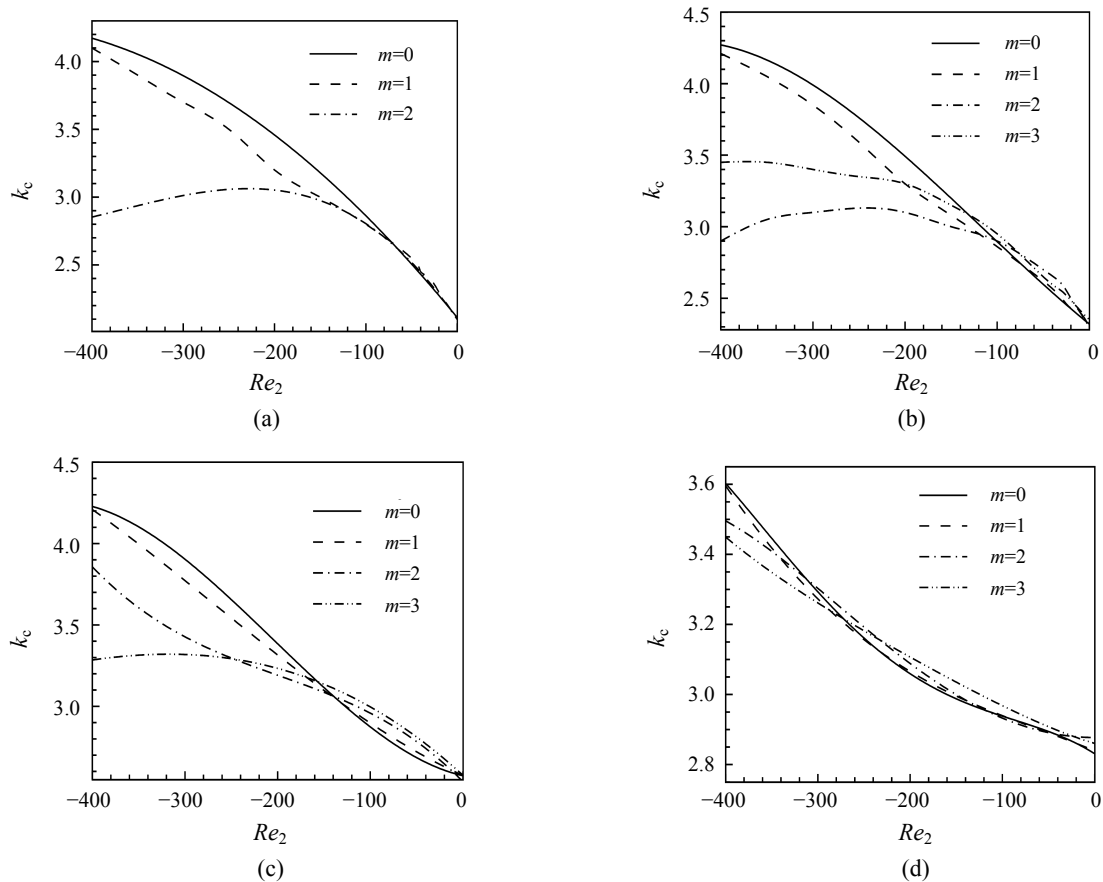


Fig.3 Relations between  $k_c$  and  $Re_2$ . (a)  $\eta=0.750$ ; (b)  $\eta=0.825$ ; (c)  $\eta=0.900$ ; (d)  $\eta=0.975$

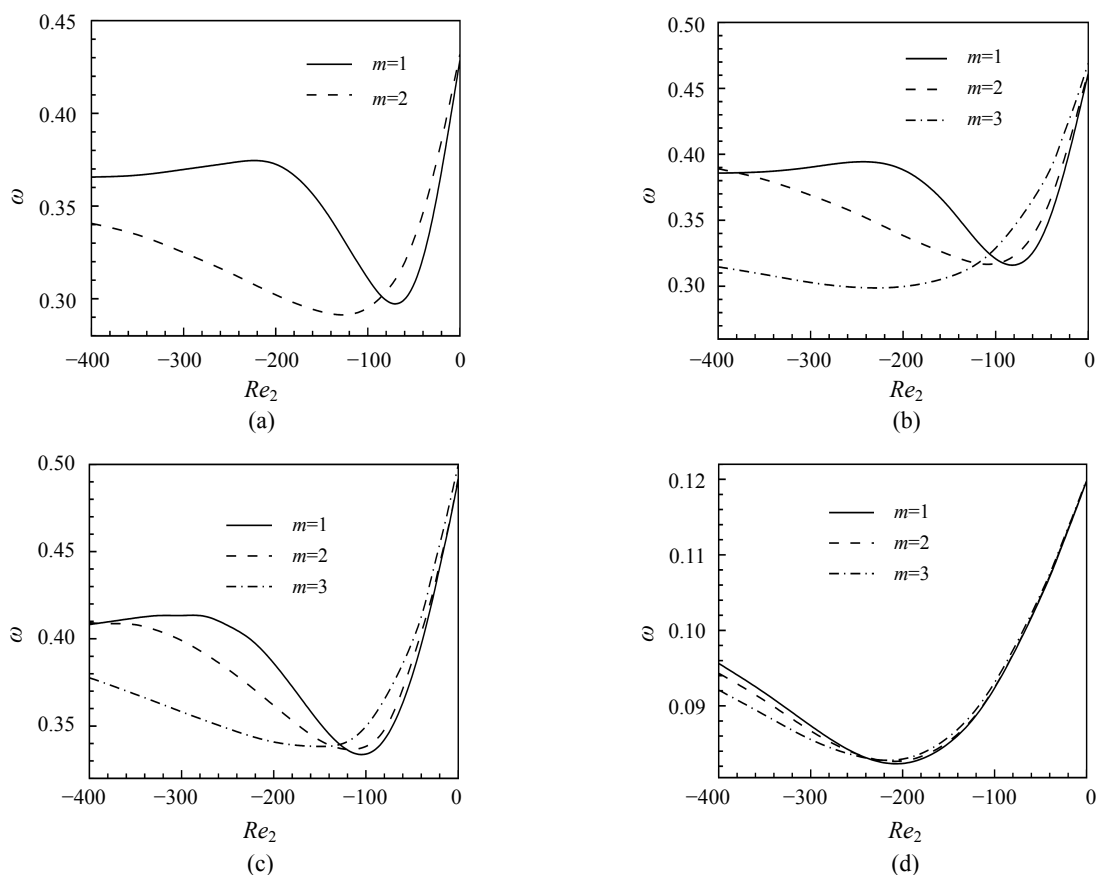


Fig.4 Relations between  $\omega$  and  $Re_2$ . (a)  $\eta=0.750$ ; (b)  $\eta=0.825$ ; (c)  $\eta=0.900$ ; (d)  $\eta=0.975$

larger than that of  $m+1$  mode. When the radii ratio tends to 1 (i.e., narrow gap situation), the wave speed of each mode is obviously smaller than that of wide gaps.

For the fixed values of the fiber parameters  $r_a$  and  $c$ , we can calculate the values of critical inner Reynolds number  $Re_c$  ( $Re_2, \eta$ ) at different azimuthal modes  $m$ . Thus, the stability curves in the three-dimensional ( $Re, Re_2, \eta$ ) parameter space are obtained. The predominant surfaces of the disturbances of instability modes are further obtained by the projection from the ( $Re, Re_2, \eta$ ) space onto the two parameters ( $Re_2, \eta$ ) and ( $Re, \eta$ ) plane, respectively. From these figures, we can find out the distribution of the most unstable disturbance modes, which are to be amplified and lead to the destabilization of the flow, in the cases of different  $\eta, Re_c$  and  $Re_2$ .

Figs.5a and 5b show the comparisons of the most unstable azimuthal modes in the flow of Newtonian fluid and fiber suspensions (aspect ratio  $r_a=10^2$ , volume fraction  $c=10^{-4}$ ), respectively. From these

figures, it is found that for a given  $\eta$ , the critical Reynolds numbers of the inner, outer cylinders  $Re_c, Re_2$  in fiber suspensions are always larger than that in Newtonian flow. The region of the high order modes in the fiber suspensions is obviously smaller than that in the Newtonian flow, i.e., the addition of the fibers attenuates the occurrence of the high order modes of the instability disturbances.

The distribution of the critical instability with aspect ratio  $r_a=10^2$  and volume fraction  $c=10^{-4}$  is given in Figs.6a and 6b. The boundaries of the regions are of special interest since it is in their vicinity that different mode interaction might be expected. In addition, analogous to the analysis of Figs.3 and 4, close to each curve, the wave speed, the axial and azimuthal wavenumbers are not generally all the same. It can be seen that all critical curves grow closer to one another with the increase of the radii ratio  $\eta$ . When  $\eta$  tends to 1, these curves almost cross each other. So the competition of multiple modes may occur in narrow gap cases. Keeping the radii ratio  $\eta$ , the value of the most

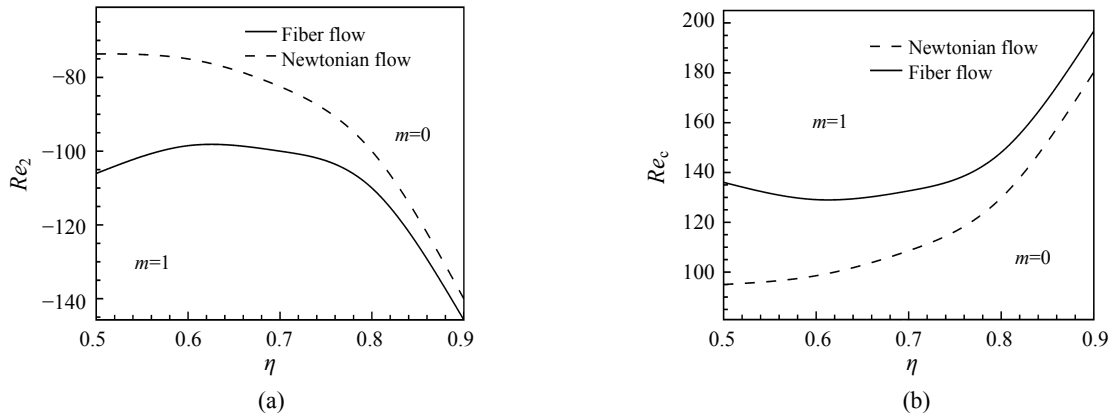


Fig.5 Comparison of bicritical curve in  $(Re_2, \eta)$  (a) and  $(Re_c, \eta)$  (b)

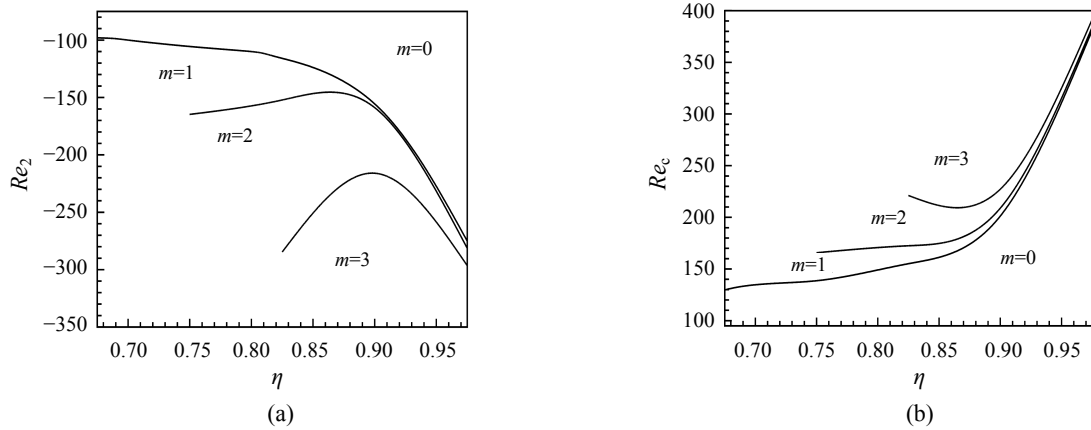


Fig.6 Bicritical curve in plane  $(Re_2, \eta)$  (a) and  $(Re_c, \eta)$  (b)

unstable azimuthal wavenumber  $m$  monotonously increases with the inner Reynolds number  $Re$  or the absolute value of the outer Reynolds number  $Re_2$ , and their spans become wider. If the value of  $\eta$  is relatively small, the most unstable azimuthal modes  $m$  change smoothly. The instability modes of the higher order azimuthal wavenumber may occur in the region where  $\eta$  is relatively large or  $Re$ ,  $Re_2$  are higher.

CONCLUSION

We have presented the results of the non-axisymmetric disturbances analysis of the Taylor-Couette flow of fiber suspensions. The constitutive model of the fiber orientation and the required closure approximation is based on the approach developed by Hinch and Leal. The comprehensive survey of the primary transition is given over a wide range of the parameters  $Re$ ,  $Re_2$ ,  $\eta$  and fiber param-

eters  $r_a$ ,  $c$ . Special attention has been focused on the bicritical curves that separate the transition from Couette flow to the flows with different azimuthal wavenumbers  $m$  and  $m+1$ . We have found that:

(1) For a specific set of fiber parameters and geometric, kinematic parameters of the flow system, the variants of the curves of the critical Reynolds number, critical axial wavenumber and wave speeds in the fiber suspensions are analogous to those of the Newtonian flow.

(2) In transition curves, the added fibers result in a stabilization effect to the flow and make the bicritical points moving towards more negative values of the outer cylinder Reynolds numbers  $Re_2$ .

(3) For a fixed azimuthal mode, the critical axial wavenumber increases with the volumic concentration and the aspect ratio of fibers.

(4) An increase of fiber parameters leads to a lower value of the wave speed of the non-axisymmetric disturbance.

(5) The presence of fibers may attenuate the occurrences of higher-order instability harmonics.

This will provide the basis for further nonlinear and experimental studies of multicritical phenomena in the Taylor-Couette flow of fiber suspensions.

## References

- Advani, S.G., Tucker III, C.L., 1987. The use of tensors to describe and predict fiber orientation in short fiber composites. *J. Rheol.*, **31**(8):751-784. [doi:10.1122/1.549945]
- Azaiez, J., 2000. Linear stability of free shear flows of fiber suspensions. *J. Fluid Mech.*, **404**:179-209. [doi:10.1017/S002211209900717X]
- Batchelor, G.K., 1971. The stress generated in a non-dilute suspension of elongated particles by pure straining motion. *J. Fluid Mech.*, **46**(4):813-829. [doi:10.1017/S0022112071000879]
- Cintra, J.S., Tucker, C.L., 1995. Orthotropic closure approximations for flow induced fiber orientation. *J. Rheol.*, **39**(6):1095-1122. [doi:10.1122/1.550630]
- Doi, M., Edwards, S.F., 1978a. Dynamics of rod-like macromolecules in concentrated solution, Part 1. *J. Chem. Soc.*, **74**:560-570.
- Doi, M., Edwards, S.F., 1978b. Dynamics of rod-like macromolecules in concentrated solution, Part 2. *J. Chem. Soc.*, **74**:918-932.
- Ericksen, J.L., 1960. Anisotropic fluids. *Arch. Rat. Mech. Anal.*, **4**:231-237.
- Ericksen, J.L., 1966. Instability in Couette flow of anisotropic fluids. *Quart. J. Mech. and Applied. Math.*, **19**(4):455-459. [doi:10.1093/qjmam/19.4.455]
- Gupta, V.K., Sureshkumar, R., Khomami, B., Azaiez, J., 2002. Centrifugal instability of semidilute non-Brownian fiber suspensions. *Phys. Fluids*, **14**(6):1958-1971. [doi:10.1063/1.1476747]
- Hand, G.L., 1962. A theory of anisotropic fluids. *J. Fluid Mech.*, **13**(1):33-46. [doi:10.1017/S0022112062000476]
- Hinch, E.J., Leal, L.G., 1975. Constitutive equations in suspension mechanics. Part 1: General formulation. *J. Fluid Mech.*, **71**(3):481-495. [doi:10.1017/S0022112075002698]
- Hinch, E.J., Leal, L.G., 1976. Constitutive equations in suspension mechanics. Part 2: Approximate forms for a suspension of rigid particles affected by Brownian rotations. *J. Fluid Mech.*, **76**(1):187-208. [doi:10.1017/S0022112076003200]
- Leslie, F.M., 1964. The stability of Couette flow of certain anisotropic fluids. *Proc. Camb. Phil. Soc.*, **60**:949-955.
- Nsom, B., 1994. Transition from circular Couette flow to Taylor vortex flow in dilute and semi-concentrated suspensions of stiff fibers. *J. Phys. II France*, **4**(1):9-22. [doi:10.1051/jp2:1994112]
- Orszag, S.A., 1971. An accurate solution of the Orr-Sommerfeld equation. *J. Fluid Mech.*, **50**(4):689-703. [doi:10.1017/S0022112071002842]
- Parsheh, M., Brown, M.L., Aidun, C.K., 2006. Investigation of closure approximations for fiber orientation distribution in contracting turbulent flow. *J. Non-Newtonian Fluid Mech.*, **136**(1):38-49. [doi:10.1016/j.jnnfm.2006.03.001]
- Pilipenko, V.N., Kalinichenko, N.M., Lemak, A.S., 1981. Stability of the flow of a fiber suspension in the gap between coaxial cylinders. *Sov. Phys. Dokl.*, **26**:646-648.
- Shaqfeh, E.S.G., Fredrickson, G.H., 1990. The hydrodynamic stress in a suspension of rods. *Physics of Fluids A: Fluid Dynamics*, **2**(1):7-24. [doi:10.1063/1.859490]
- Trefethen, L.N., 2001. Spectral Methods in MATLAB. SIAM, Philadelphia, PA.
- Verma, P.D.S., 1962. Couette flow of certain anisotropic fluids. *Arch. Rat. Mech. Anal.*, **10**(1):101-107. [doi:10.1007/BF00281179]
- Wan, Z.H., Lin, J.Z., You, Z.J., 2005. Non-axisymmetric instability in the Taylor-Couette flow of fiber suspension. *Journal of Zhejiang University SCIENCE*, **6A**(Suppl. I):1-7. [doi:10.1631/jzus.2005.AS0001]
- Wan, Z.H., Lin, J.Z., You, Z.J., 2007. Three-dimensional modes of fiber suspensions in the Taylor-Couette flow. *Journal of Dong Hua University (Eng. Ed.)*, **23**:41-47.
- Weideman, J.A.C., Reddy, S.C., 2000. A MATLAB differentiation matrix suite. *ACM Trans. Math. Softw.*, **26**(1):465-519. [doi:10.1145/365723.365727]
- You, Z.J., Lin, J.Z., Yu, Z.S., 2004. Hydrodynamic instability of fiber suspensions in channel flows. *Fluid Dyn. Res.*, **34**(4):251-271. [doi:10.1016/j.fluidyn.2004.01.002]